

Mechanism of loop-2 in facilitating microtubule depolymerase activity of kinesin-8 motors

Xiao-Xuan Shi(史晓璇), Yao Wang(王瑶), Jie Wang(王杰), Yu-Ru Liu(刘玉如), and Ping Xie(谢平)
Citation: Chin. Phys. B, 2026, 35 (**2**): 028701. DOI: 10.1088/1674-1056/adf4a8
http://cpb.iphy.ac.cn; http://iopscience.iop.org/cpb

What follows is a list of articles you may be interested in

On load dependence of detachment rate of kinesin motor

Xiao-Xuan Shi(史晓璇), Yao Wang(王瑶), Yu-Ru Liu(刘玉如), and Ping Xie(谢平)
Chin. Phys. B, 2025, 34 (**1**): 018702. DOI: 10.1088/1674-1056/ad8ec7

Origin of tradeoff between movement velocity and attachment duration of kinesin motor on a microtubule

Yuying Liu(刘玉颖) and Zhiqiang Zhang(张志强)
Chin. Phys. B, 2024, 33 (**2**): 028708. DOI: 10.1088/1674-1056/ad1177

Kinesin-microtubule interaction reveals the mechanism of kinesin-1 for discriminating the binding site on microtubule

Yi-Zhao Geng(耿轶钊), Li-Ai Lu(鲁丽爱), Ning Jia(贾宁), Bing-Bing Zhang(张冰冰), and Qing Ji(纪青)
Chin. Phys. B, 2023, 32 (**10**): 108701. DOI: 10.1088/1674-1056/acdfc1

Investigation of the structural and dynamic basis of kinesin dissociation from microtubule by atomistic molecular dynamics simulations

Jian-Gang Wang(王建港), Xiao-Xuan Shi(史晓璇), Yu-Ru Liu(刘玉如), Peng-Ye Wang(王鹏业),Hong Chen(陈洪), and Ping Xie(谢平)
Chin. Phys. B, 2022, 31 (**5**): 058702. DOI: 10.1088/1674-1056/ac598b

Protection-against-water-attack determined difference between strengths of backbone hydrogen bonds in kinesin's neck zipper region

Jing-Yu Qin(覃静宇), Yi-Zhao Geng(耿轶钊), Gang Lü(吕刚), Qing Ji(纪青), Hai-Ping Fang(方海平)
Chin. Phys. B, 2018, 27 (**2**): 028704. DOI: 10.1088/1674-1056/27/2/028704

Mechanism of loop-2 in facilitating microtubule depolymerase activity of kinesin-8 motors

Xiao-Xuan Shi(史晓璇)[1,2], Yao Wang(王瑶)[2], Jie Wang(王杰)[2], Yu-Ru Liu(刘玉如)[2], and Ping Xie(谢平)[2,†]

[1] *School of Pharmaceutical Engineering, Chongqing Chemical Industry Vocational College, Chongqing* 401220, *China*
[2] *Laboratory of Soft Matter Physics, Institute of Physics, Chinese Academy of Sciences, Beijing* 100190, *China*

(Received 29 May 2025; revised manuscript received 17 July 2025; accepted manuscript online 28 July 2025)

Kinesin-8 motors can move with a high processivity on microtubule lattices toward the plus end. After reaching the plus end, the kinesin-8 motors can pause for a long time and promote the microtubule depolymerization. Here, using atomistic molecular dynamics simulations we studied the structural changes of the kinesin-8 head in different nucleotide states bound to the straight and curved tubulins and the corresponding interactions between them. We found that the kinesin-8 head in ATP and/or ADP–Pi state has the similar strong affinity while in ADP state has the similar weak affinity to both the straight and curved tubulins, which is strongly implicated in the mechanism of the long but very different residence times of the kinesin-8 motor on the microtubule lattice and at the end. Moreover, we found that loop-2 of the kinesin-8 head bound strongly to the curved tubulin in the stable state has a large interference with its neck linker pulled in the minus-ended orientation. This is contrary to the case of the head bound strongly to the straight tubulin, where loop-2 has little interference with its neck linker pulled in the minus-ended orientation. The large interference can induce a larger internal force between the two heads and thus can induce the two curved tubulins bound strongly by the two heads to be more curved relative to each other. This is strongly implicated in the mechanism of the depolymerase activity of the kinesin-8 motors and explains the origin of loop-2 playing a facilitating role in the depolymerase activity.

Keywords: microtubule depolymerization, kinesin, binding energy, straight tubulin, curved tubulins, molecular dynamics simulation

PACS: 87.10.Tf, 87.15.A–, 87.15.hg

DOI: 10.1088/1674-1056/adf4a8 **CSTR:** 32038.14.CPB.adf4a8

1. Introduction

Kinesin molecular motors constitute a large superfamily of microtubule-associated proteins, which are involved in a variety of biological processes, including the long-distance intracellular transport of cargos, regulation of microtubule (MT) dynamics during cell mitosis, and so on.[1–4] For example, the widely-studied members of kinesin-1 family are responsible for the intracellular transport via moving processively on MT lattices toward the plus end.[1,3–6] Members of kinesin-5 families can drive relative sliding of two antiparallel MTs, playing a critical role in cell mitosis.[7] Members of kinesin-8 and kinesin-13 families are responsible for the regulation of MT dynamics via depolymerizing tubulins from the MT end.[8–17] In this work, we focus on the kinesin-8 motors.

After bound on the MT lattice, where the tubulins have the straight conformation, the kinesin-8 motors can move with a high processivity toward the plus end.[18,19] After reaching the plus end, where the tubulins have the curved conformation, the kinesin-8 motors can pause for a long time and promote MT depolymerization.[20–25] Interestingly, it was found that while multiple kinesin-8 motors accumulated at the MT plus end can promote MT depolymerization,[22] a single kinesin-8 motor at the end shows a smaller depolymerization rate than the spontaneous depolymerization rate.[26] To understand the mechanistic basis of both the processive stepping activity on the MT lattice and the depolymerase activity at the MT end of the kinesin-8 motors, a lot of experimental studies have been performed[18–26] and several models for the underlying mechanisms have been proposed.[22,24,27] Recently, the structures of the kinesin-8 Kip3 head in different nucleotide states complexed with the straight and curved tubulins were resolved using cryo-electron microscopy.[28] The structural data showed that when complexed with the straight tubulin the Kip3 head in AMP–PNP (equivalent to ATP) state has an open nucleotide-binding pocket (NBP) and an undocked neck linker (NL) while in ADP–AlF$_x$ (equivalent to ADP–Pi) state has a closed NBP and a docked NL.[28] More interestingly, when complexed with the curved tubulin the Kip3 head in AMP–PNP state has a closed NBP and a docked NL.[28] For convenience of writing, here the Kip3 head in AMP–PNP state complexed with the straight tubulin is termed as ATP–Kip3–straight-tubulin complex, the Kip3 head in ADP–AlF$_x$ state complexed with the straight tubulin is termed as ADP–Pi–Kip3–straight-tubulin complex and the Kip3 head in AMP–PNP state complexed with the curved tubulin is termed as ATP–Kip3–curved-tubulin complex. The head of kinesin-8

†Corresponding author. E-mail: pxie@aphy.iphy.ac.cn

© 2026 Chinese Physical Society and IOP Publishing Ltd. All rights, including for text and data mining, AI training, and similar technologies, are reserved.

has more elongated loop-2 regions than the head of other non-depolymerizing kinesins such as kinesin-1 and it was experimentally shown that loop-2 plays a major role in the depolymerization activity of the kinesin-8 motors.[23,24,28]

Since the kinesin head in both ATP and ADP–Pi states has the strong binding energy to straight MT[29–33] and the Kip3 head in ATP and ADP–Pi states has different conformations,[28] an interesting issue is if the Kip3 head in the ATP–Kip3–straight-tubulin complex and in the ADP–Pi–Kip3–straight-tubulin complex has similar or different binding energies to the tubulin. In order to pause at the plus end for the long time, it was usually believed that the Kip3 head has a higher binding energy to the curved tubulin at the plus end than to the straight tubulin on the MT lattice in the strong MT-binding state. However, no evidence is available to support this belief. More importantly, the detailed mechanism of the MT depolymerization promoted by kinesin-8 motors is still undetermined and in particular the origin of loop-2 playing a major role in the depolymerase activity of the kinesin-8 motors is unclear. To understand the mechanism and/or origin, besides the interactions between the kinesin-8 head and tubulin it is also necessary to study the structural change of the head bound to the tubulin. The purpose of this work is to focus on the unclear issues by using atomistic molecular dynamics (MD) simulations.

2. Methods and materials

2.1. Structures used in atomistic MD simulation

The structures of the ATP–Kip3–straight-tubulin, ADP–Pi–Kip3–straight-tubulin, and ATP–Kip3–curved-tubulin complexes were obtained from the Protein Data Bank (pdb: 7TQX, 7TQY, and 7TR3, respectively).[28] The structure of the ADP–Kip3–straight-tubulin complex is constructed based on the structural data of the Kip3 head bound with ADP (pdb: 7LFF[28]) and the tubulin taken from the ATP–Kip3–straight-tubulin complex (pdb: 7TQX[28]). The structure of the ADP–Kip3–curved-tubulin complex is constructed from the structural data of the Kip3 head bound with ADP (pdb: 7LFF[28]), and the tubulin taken from the ATP–Kip3–curved-tubulin complex (pdb: 7TR3[28]).

The structures of the ADP–Kip3–straight-tubulin and ADP–Kip3–curved-tubulin complexes are constructed via three steps, following protocols described in the previous paper.[39] First, we do molecular replacements with CHIMERA[40] as the starting model. Second, we do the energy minimizations twice. Third, the systems are equilibrated for 100 ps at 300 K and 1-bar pressure (1 bar = 10^5 Pa) in the NVT ensemble and NPT ensemble, respectively. The topology files of ADP molecule are generated by using the online PRODRG server.

2.2. Atomistic MD simulation method and data analysis

We use GROMACS4.6 with AMBER99SB force field[41] to conduct atomistic MD simulations, with the same simulation procedures and conditions as described previously[39] (seeSection S1 in supporting information for details). The analyses of HBs and SBs between the kinesin head and tubulin are described in the previous paper[39] (see Section S2 in supporting information for details).

3. Results

3.1. Kinesin-8 head has the similar strong binding energy to straight and curved tubulins

In this section, we determine if the kinesin-8 Kip3 head in the ATP–Kip3–straight-tubulin complex (pdb: 7TQX[28]), in the ADP–Pi–Kip3–straight-tubulin complex (pdb: 7TQY[28]) and in the ATP–Kip3–curved-tubulin complex (pdb: 7TR3[28]) has similar or different binding energies to the straight/curved tubulin. Firstly, we perform equilibrium MD simulations of the three complexes for 100 ns. The results for the time series of the root mean square deviation (RMSD) for C_α atoms relative to the initial ones are shown in lower panels of Fig. 1(a) and the corresponding structure of each complex at $t = 100$ ns is shown in the upper panel. As it is seen from Fig. 1(a), the three complexes reach their stable states in about 20 ns.

Then, we calculate the binding energies of the Kip3 head to the tubulin in the three complexes by using the center-of-mass (COM) pulling and umbrella sampling (see Section 2). We take the structures obtained from the MD simulations at the moment of 100 ns shown in Fig. 1(a) as the starting ones for the pulling simulations. For each complex, we obtain at least 10 curves of the pulling force versus time during the process of pulling the Kip3 head away from the tubulin (Fig. S1 in supporting information). For each complex, from the curves the median one is chosen, as shown in Figs. 2(a)–2(c). With the median curve, we calculate the change of the potential of mean force (PMF) as the function of the change in the distance (Δd) between COM position of the head and that of the tubulin for each complex using the umbrella sampling simulations. The converged results of the change of PMF versus Δd for the three complexes are plotted in Fig. 3.

From Fig. 3 it is seen that for each complex the maximum change of PMF has a high value larger than $120k_BT$, indicating that the kinesin-8 head has a very high binding energy to MT, which is consistent with the prior experimental studies showing that the kinesin-8 motor has a very small dissociation rate or a very long run length during its processive stepping on MT.[18,19] Interestingly, from Fig. 3 it is seen that the three complexes have the similar value for the maximum change of PMF. This indicates that the Kip3 head in both ATP and ADP–Pi states has the similar strong binding energy to the straight tubulin, although in ATP state the head has a very different

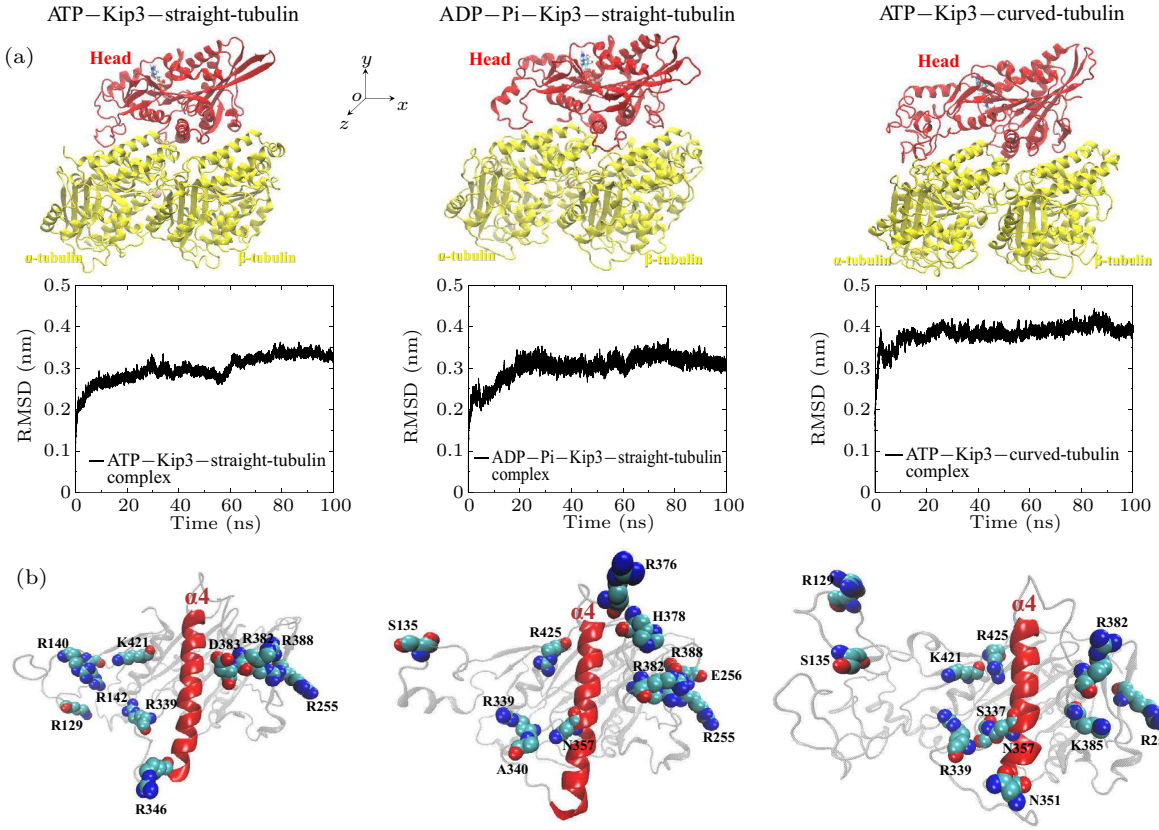


Fig. 1. Equilibrium MD simulations of interactions of the kinesin-8 Kip3 head in AMP–PNP and ADP–AlF$_x$ states with straight and curved tubulins. (a) Time series of RMSD value for the ATP–Kip3–straight-tubulin complex (left), ADP–Pi–Kip3–straight-tubulin complex (middle) and ATP–Kip3–curved-tubulin complex (right). The upper panels show the corresponding structures of the complexes at $t = 100$ ns. (b) The main residues on the head which can form HBs or SBs with those on the tubulin with the occupancy percentage for each HB or SB larger than 60% in the ATP–Kip3–straight-tubulin complex (left), ADP–Pi–Kip3–straight-tubulin complex (middle), and ATP–Kip3–curved-tubulin complex (right). The head structures shown in panel (b) are viewed from the tubulins, with MT plus end along the right direction.

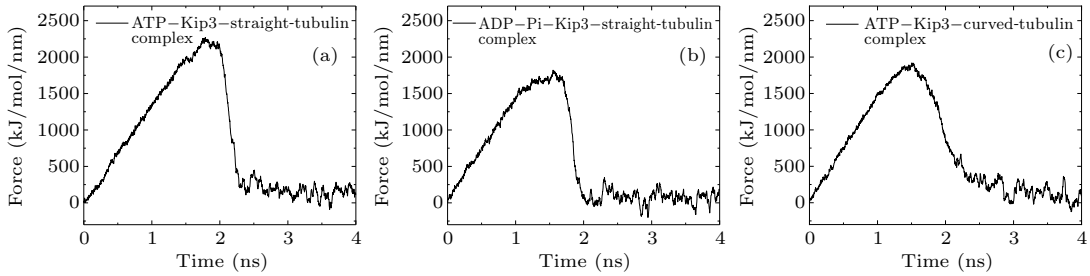


Fig. 2. The median curve of the pulling force versus time during the process of pulling the kinesin-8 Kip3 head in AMP–PNP and ADP–AlF$_x$ states away from the tubulin. The median curve is chosen from more than 10 individual curves shown in Fig. S1: (a) for the ATP–Kip3–straight-tubulin complex, (b) for the ADP–Pi–Kip3–straight-tubulin complex, (c) for the ATP–Kip3–curved-tubulin complex.

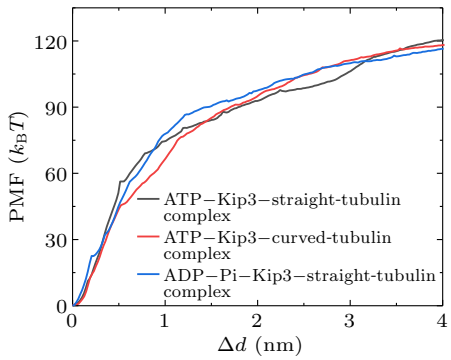


Fig. 3. The change in PMF as the function of the change in the distance (Δd) between COM position of the kinesin-8 Kip3 head and that of the tubulin for the ATP–Kip3–straight-tubulin, ADP–Pi–Kip3–straight-tubulin, and ATP–Kip3–curved-tubulin complexes.

conformation from that in ADP–Pi state, with the former conformation having the open NBP and undocked NL whereas the latter conformation having the closed NBP and docked NL. More interestingly, from Fig. 3 it is seen that the strong binding energy of the Kip3 head in ATP state to the curved tubulin and that to the straight tubulin have the similar value despite of the two tubulins having very different conformations.

3.2. Kinesin-8 head has the similar weak binding energy to straight and curved tubulins

In the above section, we have shown that the kinesin-8 head in both ATP and ADP–Pi states has the similar strong binding energy to the straight/curved tubulin. Prior structural

data showed that ATP can bind to both the trailing and leading heads.[34] Thus, at physiological or saturating ATP concentration, it can be considered that an ATP can bind to the nucleotide-free head instantly, implying that the nucleotide-free state is not necessary to be considered. Thus, to explore if the large difference between the residence time of the kinesin-8 motor on the MT lattice and that at the MT plus end arises from the evident difference between the binding energies of the kinesin-8 head in various nucleotide-bound states to the straight tubulin and the corresponding ones to the curved tubulin, it is also interesting to determine the weak binding energy of the kinesin-8 head in ADP state to the straight tubulin and that to the curved tubulin.

We construct two complexes of a Kip3 head in ADP state (pdb: 7LFF[28]) bound with a tubulin (see Section 2). In one complex the ADP-head is bound to the straight tubulin (taken from pdb: 7TQX[28]), called ADP–Kip3–straight-tubulin complex, and in another one the ADP-head is bound to the curved tubulin (taken from pdb: 7TR3[28]), called ADP–Kip3–curved-tubulin complex. We perform equilibrium MD simulations of the two complexes for 100 ns. The results for the time series of the RMSD for C_α atoms relative to the initial ones are shown in lower panels of Fig. 4(a) and the corresponding structure of each complex at $t = 100$ ns is shown in the upper panel. As it is seen from Fig. 4(a), the two complexes reach their stable states in about 10 ns.

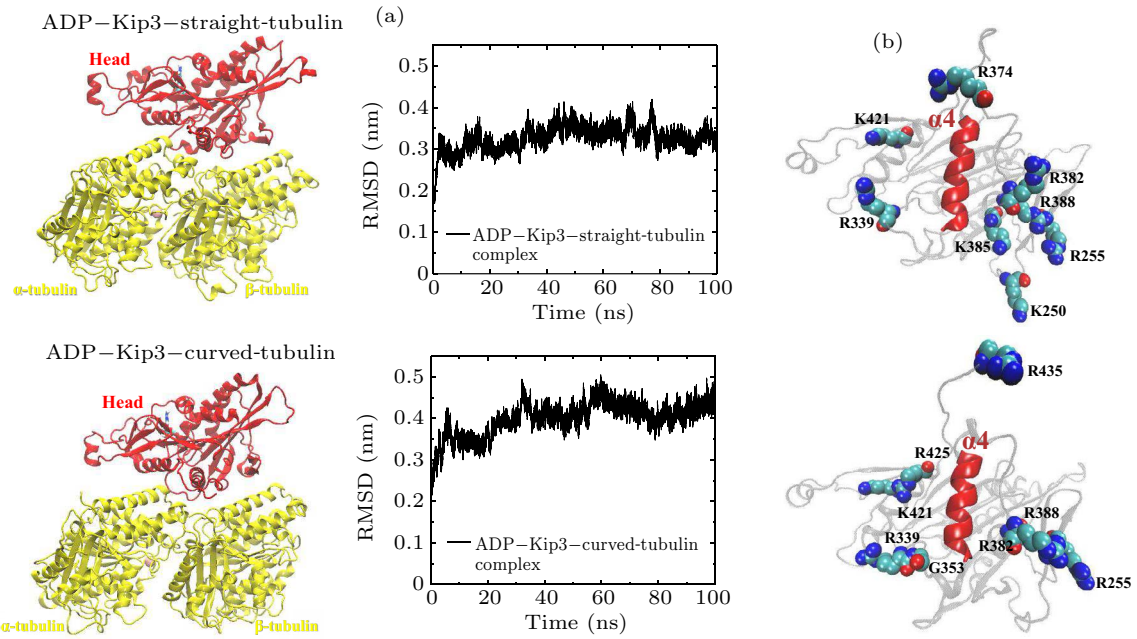


Fig. 4. Equilibrium MD simulations of interactions of the kinesin-8 Kip3 head in ADP state with straight and curved tubulins. (a) Time series of RMSD value for the ADP–Kip3–straight-tubulin complex (left) and ADP–Kip3–curved-tubulin complex (right). The upper panels show the corresponding structures of the complexes at $t = 100$ ns. (b) The main residues on the head which can form HBs or SBs with those on the tubulin with the occupancy percentage for each HB or SB larger than 60% in the ADP–Kip3–straight-tubulin complex (left) and ADP–Kip3–curved-tubulin complex (right). The head structures shown in panel (b) are viewed from the tubulins, with MT plus end along the right direction.

We take the structures obtained from the MD simulations at the moment of 100 ns shown in Fig. 4(a) as the starting ones for the pulling simulations. For each complex, we obtain at least 10 curves of the pulling force versus time during the process of pulling the Kip3 head away from the tubulin (Fig. S2 in supporting information). For each complex, from the curves the median one is chosen, as shown in Fig. 5. With the median curve, we calculate the change of PMF as the function of the change in the distance (Δd) between COM position of the head and that of the tubulin for each complex. The converged results of the change of PMF versus Δd for the two complexes are shown in Fig. 6.

Comparing Fig. 6 with Fig. 3, it is seen that the value for the maximum change of PMF for the ADP–Kip3–straight-tubulin or ADP–Kip3–curved-tubulin complex is evidently smaller than that for the ATP–Kip3–straight-tubulin, ADP–Pi–Kip3–straight-tubulin or ATP–Kip3–curved-tubulin complex. This is consistent with the common belief that like kinesin-1, the kinesin-8 in ADP state has the weak binding energy to MT while in ATP and ADP–Pi state has the strong binding energy. More interestingly, from Fig. 6 it is seen the ADP–Kip3–straight-tubulin and ADP–Kip3–curved-tubulin complexes have the similar value for the maximum change of PMF. This indicates that the weak binding energy of the Kip3 head in ADP state to the curved tubulin and that to the straight tubulin have the similar value.

Taken together, the results in this section and those in the above section show that the kinesin-8 head in ATP and/or ADP–Pi state has the similar strong binding energy to the straight and curved tubulins while in ADP state has the similar weak binding energy to the straight and curved tubulins. This implies that the evidently distinct residence times of the

kinesin-8 motor on the MT lattice and at the MT end is not due to the different binding energies of the kinesin to the tubulins of different conformations (see Section 4).

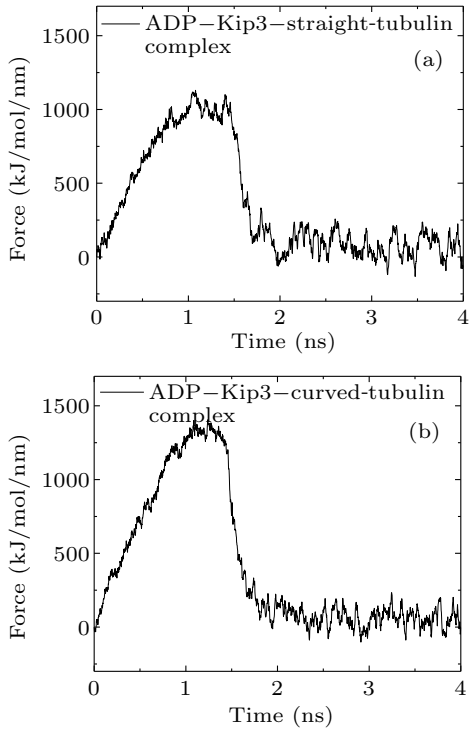


Fig. 5. The median curve of the pulling force versus time during the process of pulling the kinesin-8 Kip3 head in ADP state away from the tubulin. The median curve is chosen from more than 10 individual curves shown in Fig. S2. (a) For the ADP–Kip3–straight-tubulin complex. (b) For the ADP–Kip3–curved-tubulin complex.

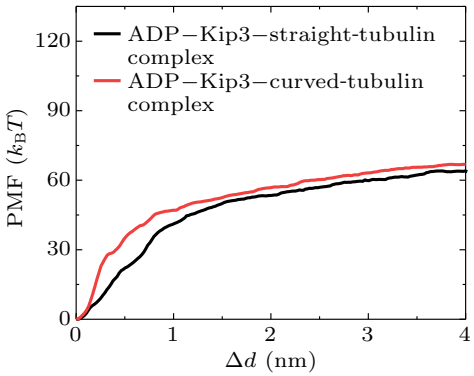


Fig. 6. The change in PMF as the function of the change in the distance (Δd) between COM position of the kinesin-8 Kip3 head and that of the tubulin for the ADP–Kip3–straight-tubulin and ADP–Kip3–curved-tubulin complexes.

3.3. Kinesin-8 head has distinct interacting residues with straight and curved tubulins

In this subsection, we analyze statistically the main interacting residues on the kinesin head with the tubulin in the ATP–Kip3–straight-tubulin, ADP–Pi–Kip3–straight-tubulin, ATP–Kip3–curved-tubulin, ADP–Kip3–straight-tubulin, and ADP–Kip3–curved-tubulin complexes. The statistical analyses are performed based on the simulation trajectories of the five complexes in the time period between 50 ns and 100 ns (Figs. 1 and 4). We calculate the hydrogen-bond and salt-bridge occupancy percentage for each interacting residue pair between the kinesin head and tubulin. The residues on the head which can form hydrogen bonds (HBs) or salt bridges (SBs) with those on the tubulin with the occupancy percentage for each HB or SB larger than 60% in the ATP–Kip3–straight-tubulin, ADP–Pi–Kip3–straight-tubulin, and ATP–Kip3–curved-tubulin complexes are shown in Fig. 1(b). The corresponding description of the residues shown in Fig. 1(b) is given in Table 1. The residues on the head which can form HBs or SBs with those on the tubulin with the occupancy percentage for each HB or SB larger than 60% in the ADP–Kip3–straight-tubulin and ADP–Kip3–curved-tubulin complexes are shown in Fig. 4(b). The corresponding description of the residues shown in Fig. 4(b) is given in Table 2.

From Fig. 1(b) and Table 1, it is interesting to see that the main residues on the head which can interact with the tubulin in the ATP–Kip3–straight-tubulin, ADP–Pi–Kip3–straight-tubulin, and ATP–Kip3–curved-tubulin complexes are different, although the binding energies of the head to the tubulin are similar for the three complexes (Fig. 3). More interestingly, from Fig. 1(b) it is noted that the tubulin-interacting residues on or near the α4 helix in the ADP–Pi–Kip3–straight-tubulin complex are more similar to those in the ATP–Kip3–curved-tubulin complex than to those in the ATP–Kip3–straight-tubulin complex. In other words, although in the ADP–Pi–Kip3–straight-tubulin and ATP–Kip3–curved-tubulin complexes the Kip3 head has different nucleotide states (ADP–Pi state in the former whereas ATP state in the latter), the tubulin-interacting residues on or near the α4 helix in the two complexes are similar and the head in the two complexes has the similar conformation with closed NBP and docked NL. Although in the ATP–Kip3–straight-tubulin and ATP–Kip3–curved-tubulin complexes the Kip3 head has the same nucleotide state (ATP state in both complexes), the tubulin-interacting residues on or near the α4 helix in the two complexes are different and the head in the two complexes has different conformations, with the former having open NBP and undocked NL whereas the latter having closed NBP and docked NL. These thus imply that it is the different tubulin-interacting residues on or near the α4 helix that can induce the head in the ADP–Pi–Kip3–straight-tubulin and ATP–Kip3–curved-tubulin complexes to have the large conformational change associated with NBP closing and NL docking whereas the head in the ATP–Kip3–straight-tubulin to be unable to make the large conformational change.

From Fig. 4(b) and Table 2, it is also seen that the main tubulin-interacting residues on the head between the ADP–Kip3–straight-tubulin and ADP–Kip3–curved-tubulin complexes are very different, although the binding energies of the head to the tubulin are similar for the two complexes.

Table 1. Description of the residues on kinesin-8 head (shown in Fig. 1(b)) which form hydrogen bonds (HBs) or salt bridges (SBs) with tubulin in the ATP–Kip3–straight-tubulin, ADP–Pi–Kip3–straight-tubulin, and ATP–Kip3–curved-tubulin complexes. Only interactions with occupancy percentage greater than 60% are listed.

System	Residue	HB & SB number	Detailed description
ATP–Kip3–straight-tubulin complex	ARG255	HBs: 3, SBs: 3	1st-HB(182.23%), 2nd-HB(82.74%), 3rd-HB(74.64%); 1st-SB(100.00%), 2nd-SB(99.56%), 3rd-SB(95.54%)
ATP–Kip3–straight-tubulin complex	ARG140	HBs: 1, SBs: 2	1st-HB(218.82%); 1st-SB(99.86%), 2nd-SB(65.27%)
ATP–Kip3–straight-tubulin complex	ASP383	HBs: 1, SBs: 1	1st-HB(229.32%); 1st-SB(99.99%)
ATP–Kip3–straight-tubulin complex	ARG346	HBs: 1, SBs: 1	1st-HB(139.70%); 1st-SB(70.56%)
ATP–Kip3–straight-tubulin complex	ARG382	HBs: 1, SBs: 1	1st-HB(95.73%) ;1st-SB(99.70%)
ATP–Kip3–straight-tubulin complex	ARG129	HBs: 2, SBs: 0	1st-HB(103.60%), 2nd-HB(72.12%)
ATP–Kip3–straight-tubulin complex	ARG142	HBs: 1, SBs: 1	1st-HB(67.01%); 1st-SB(73.79%)
ATP–Kip3–straight-tubulin complex	ARG339	HBs: 0, SBs: 1	1st-SB(100.00%)
ATP–Kip3–straight-tubulin complex	ARG388	HBs: 0, SBs: 1	1st-SB(99.49%)
ATP–Kip3–straight-tubulin complex	LYS421	HBs: 1, SBs: 0	1st-HB(64.99%)
ADP–Pi–Kip3–straight-tubulin complex	ARG255	HBs: 1, SBs: 2	1st-HB(216.33%); 1st-SB(99.88%), 2nd-SB(75.95%)
ADP–Pi–Kip3–straight-tubulin complex	ARG382	HBs: 1, SBs: 1	1st-HB(265.24%); 1st-SB(100.00%)
ADP–Pi–Kip3–straight-tubulin complex	ARG376	HBs: 2, SBs: 1	1st-HB(95.79%), 2nd-HB(80.44%); 1st-SB(79.57%)
ADP–Pi–Kip3–straight-tubulin complex	ARG388	HBs: 1, SBs: 2	1st-HB(77.21%); 1st-SB(99.96%), 2nd-SB(70.65%)
ADP–Pi–Kip3–straight-tubulin complex	ARG339	HBs: 0, SBs: 2	1st-SB(99.92%), 2nd-SB(97.61%)
ADP–Pi–Kip3–straight-tubulin complex	ALA340	HBs: 2, SBs: 0	1st-HB(84.37%), 2nd-HB(81.75%)
ADP–Pi–Kip3–straight-tubulin complex	SER135	HBs: 1, SBs: 0	1st-HB(86.94%)
ADP–Pi–Kip3–straight-tubulin complex	ARG425	HBs: 0, SBs: 1	1st-SB(74.92%)
ADP–Pi–Kip3–straight-tubulin complex	GLU256	HBs: 1, SBs: 0	1st-HB(71.13%)
ADP–Pi–Kip3–straight-tubulin complex	ASN357	HBs: 1, SBs: 0	1st-HB(64.56%)
ADP–Pi–Kip3–straight-tubulin complex	HIS378	HBs: 1, SBs: 0	1st-HB(60.83%)
ATP–Kip3–curved-tubulin complex	ARG255	HBs: 2, SBs: 2	1st-HB(155.60%), 2nd-HB(78.34%); 1st-SB(95.65%), 2nd-SB(91.84%)
ATP–Kip3–curved-tubulin complex	LYS421	HBs: 1, SBs: 2	1st-HB(80.84%);1st-SB(99.41%); 2nd-SB(87.55%)
ATP–Kip3–curved-tubulin complex	ARG425	HBs: 1, SBs: 1	1st-HB(168.31%); 1st-SB(96.50%)
ATP–Kip3–curved-tubulin complex	ARG382	HBs: 1, SBs: 2	1st-HB(78.43%);1st-SB(92.16%), 2nd-SB(62.86%)
ATP–Kip3–curved-tubulin complex	SER337	HBs: 1, SBs: 0	1st-HB(115.39%)
ATP–Kip3–curved-tubulin complex	SER135	HBs: 1, SBs: 0	1st-HB(107.82%)
ATP–Kip3–curved-tubulin complex	ARG339	HBs: 0, SBs: 1	1st-SB(99.95%)
ATP–Kip3–curved-tubulin complex	LYS385	HBs: 0, SBs: 1	1st-SB(91.82%)
ATP–Kip3–curved-tubulin complex	ARG129	HBs: 1, SBs: 0	1st-HB(70.16%)
ATP–Kip3–curved-tubulin complex	ASN351	HBs: 1, SBs: 0	1st-HB(68.17%)
ATP–Kip3–curved-tubulin complex	ASN357	HBs: 1, SBs: 0	1st-HB(64.23%)

Table 2. Description of the residues on kinesin-8 head (shown in Fig. 4(b)) which form hydrogen bonds (HBs) or salt bridges (SBs) with tubulin in the ADP–Kip3–straight-tubulin and ADP–Kip3–curved-tubulin complexes. Only interactions with occupancy percentage greater than 60% are listed.

System	Residue	HB & SB number	Detailed description
ADP–Kip3–straight-tubulin complex	ARG255	HBs: 1, SBs: 2	1st-HB(207.82%); 1st-SB(99.76%), 2nd-SB(89.16%)
ADP–Kip3–straight-tubulin complex	ARG388	HBs: 1, SBs: 1	1st-HB(197.76%); 1st-SB(100.00%)
ADP–Kip3–straight-tubulin complex	ARG382	HBs: 1, SBs: 1	1st-HB(190.60%); 1st-SB(97.88%)
ADP–Kip3–straight-tubulin complex	LYS421	HBs: 1, SBs: 1	1st-HB(63.31%); 1st-SB(82.99%)
ADP–Kip3–straight-tubulin complex	ARG339	HBs: 0, SBs: 1	1st-SB(97.94%)
ADP–Kip3–straight-tubulin complex	LYS385	HBs: 0, SBs: 1	1st-SB(72.87%)
ADP–Kip3–straight-tubulin complex	ARG374	HBs: 1, SBs: 0	1st-HB(62.42%)
ADP–Kip3–straight-tubulin complex	LYS250	HBs: 0, SBs: 1	1st-SB(60.60%)
ADP–Kip3–curved-tubulin complex	LYS421	HBs: 2, SBs: 2	1st-HB(110.66%), 2nd- HB(82.35%) ; 1st-SB(99.93%), 2nd-SB(92.05%)
ADP–Kip3–curved-tubulin complex	ARG388	HBs: 1, SBs: 1	1st-HB(173.22%); 1st-SB(98.82%)
ADP–Kip3–curved-tubulin complex	ARG255	HBs: 1, SBs: 1	1st-HB(167.67%); 1st-SB(91.40%)
ADP–Kip3–curved-tubulin complex	ARG435	HBs: 1, SBs: 1	1st-HB(161.62%); 1st-SB(80.90%)
ADP–Kip3–curved-tubulin complex	ARG382	HBs: 1, SBs: 1	1st-HB(113.73%); 1st-SB(92.81%)
ADP–Kip3–curved-tubulin complex	ARG339	HBs: 0, SBs: 2	1st-SB(98.01%), 2nd-SB(97.05%)
ADP–Kip3–curved-tubulin complex	ARG425	HBs: 1, SBs: 1	1st-HB(78.29%) ; 1st-SB(98.75%)
ADP–Kip3–curved-tubulin complex	GLY353	HBs: 1, SBs: 0	1st-HB(77.17%)

From Figs. 1(b) and 4(b), we see that among the five complexes only the tubulin-interacting residues on or near the α4 helix in the ADP–Pi–Kip3–straight-tubulin and ATP–Kip3–curved-tubulin complexes are similar, whereas the tubulin-interacting residues on or near the α4 helix in other three complexes are very different from those in the ADP–Pi–Kip3–straight-tubulin or ATP–Kip3–curved-tubulin complex. On the other hand, it is noted that in the ADP–Pi–Kip3–straight-tubulin and ATP–Kip3–curved-tubulin complexes the head has the large conformational change associated with the NBP closing and NL docking whereas in other three complexes the head has no the large conformational change associated with the open NBP and undocked NL.[28] Therefore, we conclude that it is the tubulin-interacting residues on or near the α4 helix rather than the nucleotide-bound state that can induce the large conformational change of the head together with the NBP closing and NL docking.

3.4. Loop-2 of kinesin-8 head bound to curved tubulin interferes largely with its NL pulled in the minus-ended orientation

In this section, we investigate the structural changes of the Kip3 head in the ATP–Kip3–straight-tubulin, ADP–Pi–Kip3–straight-tubulin, and ATP–Kip3–curved-tubulin complexes (Fig. 7). Our simulations show that in the ATP–Kip3–straight-tubulin and ADP–Pi–Kip3–straight-tubulin complexes loop-2 makes the clockwise rotation whereas in the ATP–Kip3–curved-tubulin complex loop-2 makes the counterclockwise rotation (viewed from the kinesin-8 head toward tubulin and indicated by green arrows in the lower panels of Fig. 7(b)). Interestingly, it is noted even in the initial structures while loop-2 in the ATP–Kip3–straight-tubulin and ADP–Pi–Kip3–straight-tubulin complexes has no interference effect on the NL if it is pulled in the backward orientation (along the $-x$ direction), loop-2 in the ATP–Kip3–curved-tubulin complex has an interference effect on the NL if it is pulled in the backward

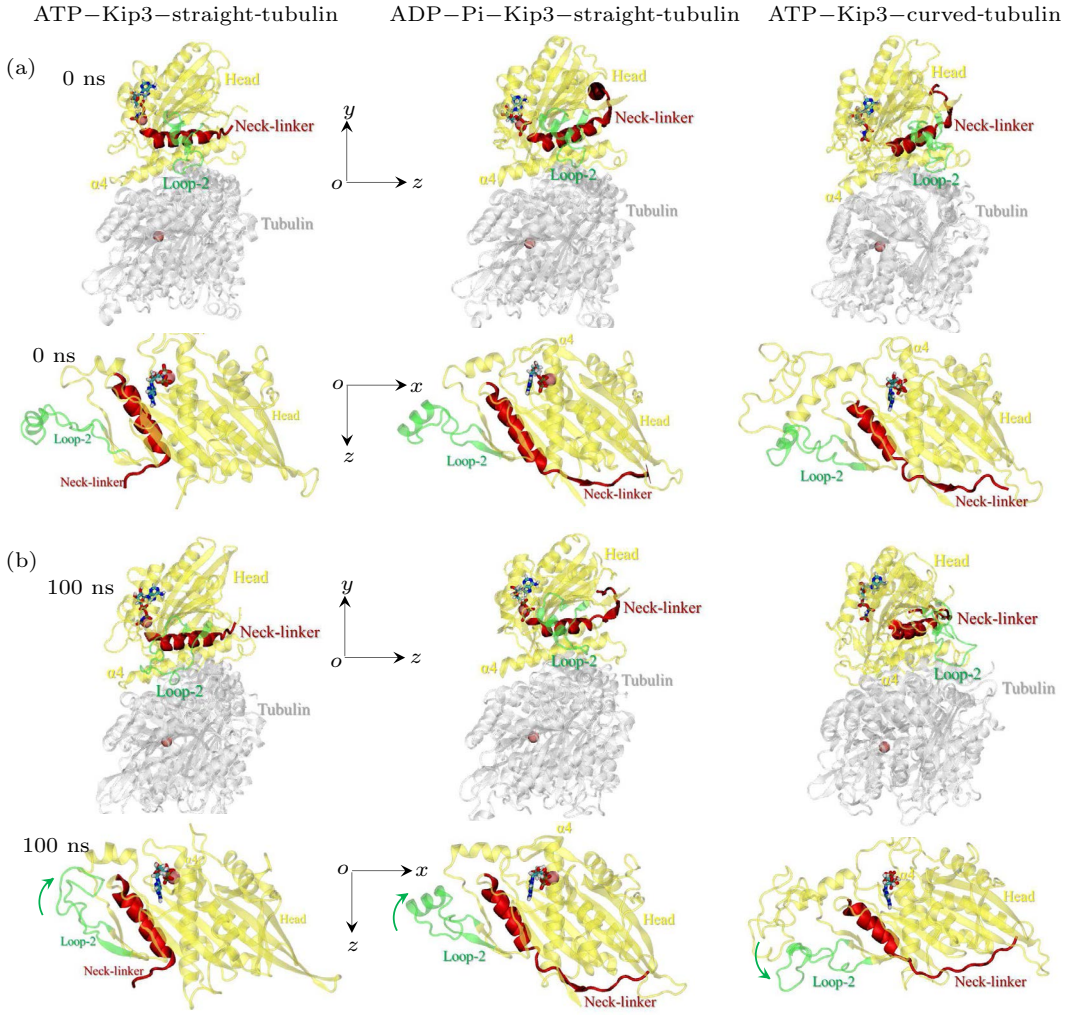


Fig. 7. Comparisons of the structures of the ATP–Kip3–straight-tubulin complex (left), ADP–Pi–Kip3–straight-tubulin complex (middle), and ATP–Kip3–curved-tubulin complex (right) at the finally stable state with those at the initial state. (a) The structures at the initial state, namely, at 0 ns. (b) The structures at the finally stable state, namely, at $t = 100$ ns. In panels (a) and (b), the upper panels correspond to the structures viewed along the plus-ended direction and the lower panels correspond to the vertical views of the upper panels after making a clockwise 90° rotation, where for clarity in the vertical views only the kinesin-8 heads are shown. Loop-2 is drawn in green. Green arrows in the lower panels of panel (b) represent the rotation direction of loop-2 in the finally stable state relative to the initial state. Only in the ATP–Kip3–curved-tubulin complex loop-1 is drawn in blue.

orientation (Fig. 7(a)). More interestingly, it is noted that in the finally stable state the counterclockwise rotation of loop-2 in the ATP–Kip3–curved-tubulin complex can enhance largely the interference of loop-2 on the NL if it is pulled in the backward orientation (Fig. 7(b) and Fig. S3 in supporting information). Note that residues in loop-2 such as S135 and R129 have strong interactions with tubulin, as seen from Fig. 1(b) for the ATP–Kip3–curved-tubulin complex. This ensures that loop-2 in the Kip3-tubulin complex is not flexible and cannot move stochastically, which can be seen from Fig. S4 and movie 1 (see supporting information). In Fig. S4 we show a series of snapshots of the Kip3 structure in the ATP–Kip3–curved-tubulin complex after 60-ns simulations and in movie 1 we show the temporal evolution of the Kip3 structure in the ATP–Kip3–curved-tubulin complex (from 0 ns to 100 ns).

As the finally stable structures are more representative of the actual situation than the initial structures, from above simulation results we thus have following conclusion. For the kinesin-8 dimer with its two heads in both ATP and ADP–Pi states bound to the straight tubulins on the MT lattice, namely, in the two-heads-bound (2HB) state of the dimer on the MT lattice, loop-2 of the leading head has no interference effect on the NL that is stretched in the backward orientation. By contrast, in the 2HB state of the kinesin-8 dimer near the MT plus end, loop-2 of the leading head has a large interference effect on the NL that is stretched in the backward orientation. The large interference at the plus end, compared to the lack of interference on the lattice, implies that for the dimer in the 2HB state near the MT plus end, the total length of the two stretched NLs will be increased largely relative to that on the MT lattice.

3.5. Kinesin-8 dimer bound to two curved tubulins at MT end generates a larger internal force between the two heads than bound to two straight tubulins on MT lattice

As it is noted, when the kinesin-8 motor is in the 2HB state, with the two heads bound to successive tubulins that is about 8.2 nm apart on an MT filament, the two NLs are required to be stretched due to the NL of the kinesin-8 head having a short length of 17 residues. As our results shown in the above section, in the 2HB state of the kinesin-8 motor on the MT lattice, no interference is present on the two stretched NLs, implying that each NL is required to have a stretched length of about 4.1 nm. By contrast, in the 2HB state of the kinesin-8 motor near the MT plus end, due to the large interference of loop-2 on the NL of the leading head that is stretched in the backward orientation, each NL is required to have a stretched length that is larger than 4.1 nm. Here, using atomistic MD simulation method (see Section S1 in the supporting information), we calculate the force required to stretch the NL of the kinesin-8 head. In Fig. 8 we show the simulation results of the stretching force versus the length of the stretched NL (dots). The simulation data can be well fitted using the 'revised complete worm-like chain' (RC-WLC) model[35] (red solid line). From Fig. 8, it is seen that for the kinesin-8 motor on the MT lattice, the internal force on the two heads, which is equal to the stretching force at the length of 4.1 nm (vertical dashed line), is about 20 pN (horizontal dashed line). At the length larger than 4.1 nm, the force increases quickly with the increase of the length. This implies that for the kinesin-8 motor near the MT plus end, the internal force on the two heads would be larger than 20 pN. The large internal force (>20 pN) on the two heads can produce a large backward force (F) of the same magnitude on the upper surface of the front curved tubulin (e.g., the first tubulin from the MT plus end), where the leading head and the tubulin interact strongly with each other, and correspondingly a large forward force of the same magnitude on the upper surface of the rear (the second) curved tubulin (the inset of Fig. 8). As will be discussed in Section 4, the two large opposite forces on the upper surfaces of the two adjacent curved tubulins can make the tubulins be more curved relative to each other, implicating strongly in the mechanism of the depolymerase activity of the kinesin-8 motors (see next section).

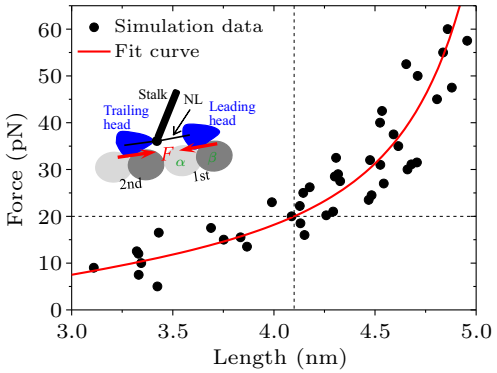


Fig. 8. Stretching force versus the length of the stretched NL. Dots represent the simulation data and the line is the fit to the simulation data using the 'revised complete worm-like chain' (RC-WLC) model (see Section S3 in supporting information). The vertical dashed line indicates the length (4.1 nm) of the stretched NL of one head in the 2HB state if loop-2 has no interference with the NL. The horizontal dashed line indicates the stretched force (20 pN) on the NL at the length of 4.1 nm. Note that the horizontal dashed line, vertical dashed line, and red solid line intersect at the same point. When loop-2 has the interference with the stretched NL, the large internal force (>20 pN) on the two heads can produce a large backward force (F) of the same magnitude on the upper surface of the front curved tubulin (e.g., the first tubulin from the MT plus end), and correspondingly a large forward force of the same magnitude on the upper surface of the rear (the second) curved tubulin, which is shown schematically in the inset.

4. Discussion

4.1. Origin of different residence times of kinesin-8 motor on MT lattice and at plus end

The available experimental data showed that the velocity of kinesin-8 Kip3 is about 42 nm/s and the run length is

about 12.4 μm,[18,19] implying that the residence time of the motor is about 300 s on the MT lattice, while the experimental data gave the residence time of about 77 s at the MT plus end.[22] A simple and direct explanation for these different residence times is due to different binding energies of the motor to straight versus curved tubulins. An alternative explanation of the origin for the different residence times of the kinesin-8 motor is that the motor shows different pathways of the chemomechanical coupling on the MT lattice and at the MT plus end but having the similar nucleotide-dependent binding energy to the straight and curved tubulins.[36] The different pathways are due solely to the fact that on the MT lattice the tubulin in the front of the motor is present whereas no front tubulin is present when the motor is at the plus end. On the MT lattice, after the detachment of the trailing ADP-head and the NL docking of the MT-bound ATP–Pi-head the detached ADP-head can bind rapidly to the front tubulin. This thus results in the motor to have a very small probability to dissociate during the very short time period after the detachment of the trailing head and before the binding of the detached head to the front tubulin. By contrast, at the MT plus end, after the detachment of the trailing ADP-head, due to the NL docking of the MT-bound ATP–Pi-head, the detached head takes a longer time to rebind to the rear head. This thus results in the motor to have a larger probability to dissociate during the longer time period after the detachment of the trailing head and before the rebinding of the detached head to the rear tubulin. Here, using atomistic MD simulations we showed that the kinesin-8 head has the similar strong and weak binding energies to the straight and curved tubulins. This argues against the former explanation, because even assuming that at the MT plus end the ATPase activity is suppressed and the motor is always in the strong MT-binding state it would be expected that the residence time at the MT end is longer than on the MT lattice. By contrast, our results support the latter explanation that the different residence times of the kinesin-8 motor on the MT lattice and at the MT end arise from the different chemomechanical pathways.

4.2. Molecular mechanism of depolymerase activity of kinesin-8 motors

As previous biochemical data showed,[23,24,28] loop-2 is a critical element to promote the depolymerase activity of the kinesin-8 motors. Here, we show that in the 2HB state of the dimer near the MT plus end loop-2 of the leading head has a large interference effect on the NL that is stretched in the backward orientation. This thus induces two large opposite forces of the same magnitude on the upper surfaces of the two adjacent tubulins near the MT plus end (Fig. 8). The two large opposite forces can induce the large curvature of one tubulin relative to the other one.[27] In addition, the prior structural analysis indicated that the closed conformation of the kinesin-8 head is accompanied by slight tubulin structural changes toward the curved conformation.[28] On the basis of these two pieces of evidence, the model for the mechanism and the origin of loop-2 playing a facilitating role in the MT depolymerase activity of kinesin-8 motors at the MT end can be explained, as described as follows.

Firstly, consider a single kinesin-8 bound to the first and second tubulins that are counted from the plus end of an MT filament (Fig. 9(a)).[27] Although the large relative curvature between the two tubulins induced by the motor bound to them can result in the first tubulin to deviate its position largely from that with no motor bound to the two tubulins, the position of the second tubulin can be changed slightly relative to that with no motor bound to the two tubulins, because the plus end of the first tubulin is free whereas both ends of the second tubulin are not free. This decreases the lateral interaction of the first tubulin with the two adjacent tubulins in the two adjacent filaments. Thus, the rate of the removal of the first tubulin is increased evidently relative to that with no motor bound to the first tubulin, while the rate of the removal of the first and second tubulin is increased slightly. After the removal of the first tubulin, since the first tubulin bound by the leading head of the motor can only be fluctuated around the second tubulin, the first tubulin can be reassembled rapidly. This can thus result in the removal rate of the first tubulin to be smaller than that in the absence of the motor bound to the MT, which is consistent with the available experimental data.[26]

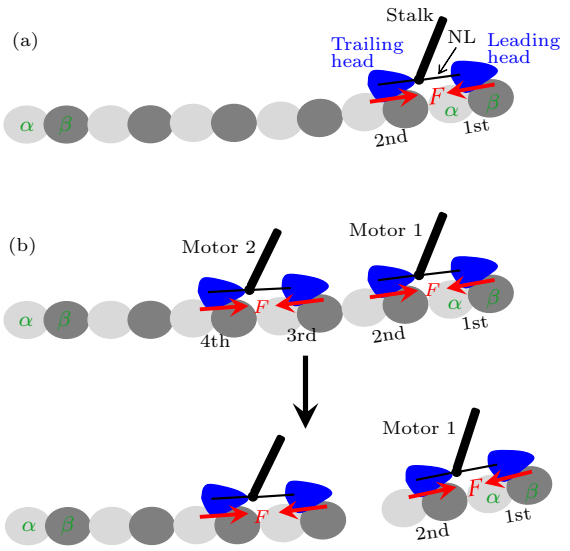


Fig. 9. Schematic illustrations of the model of MT depolymerization promoted by kinesin-8 motors. For clarity, only a single filament of the MT is drawn and only the additional bending of the filament induced by the internal force between the two heads of the motor is shown. (a) A single motor at the plus end can stabilize MT. (b) MT depolymerization promoted by two motors at the plus end of the filament.

Secondly, consider one kinesin-8 (motor 1) bound to the first and second tubulins and another kinesin-8 (motor 2) bound to the third and fourth tubulins (Fig. 9(b)).[27] Motor 1 bound to the first and second tubulins induces the large relative curvature between the two tubulins. This induces the first tubulin to deviate its position largely from that when no motor is bound to the two tubulins. Motor 2 bound to the third and fourth tubulins induces the large relative curvature between the two tubulins. This induces the third tubulin to deviate its position largely from that when no motor is bound to the two tubulins, in turn inducing the first and second tubulin to deviate their positions largely from those when no motor is bound to the third and fourth tubulins. This decreases largely the lateral interaction of the first and second tubulins with the adjacent tubulins in the two adjacent filaments. Thus, the rate of the removal of the first and second tubulins is increased largely relative to that in the absence of motors bound to the MT. It is noted that this promotion of the depolymerization by kinesin-8 motors is via a mechanism of making the MT filaments near the plus end more curved. This is similar to the case with the application of a pushing force on the plus end of MT,[37] where it was shown that under no pushing force the MT is polymerized at its plus end and under the pushing force larger than 3 pN the MT is depolymerized, with the depolymerase rate increasing with the increase of the pushing force. The removal of the first and second tubulins is accompanied by the detachment of the motor bound to them from MT, implying that the depolymerase activity of the kinesin-8 motor is nonprocessive. This is consistent with the available experiments demonstrating that multiple kinesin-8 motors at the MT plus end can promote greatly the depolymerase rate.[22]

Thirdly, consider a truncated monomeric kinesin-8 bound to the first tubulin from the plus end. The closure of the monomeric kinesin-8 induced by ATP binding is accompanied by slight tubulin structural changes toward the curved conformation, as prior structural analysis showed.[28] This results in the first tubulin to deviate its position from that when no monomer is bound to it, decreasing the lateral interaction of the first tubulin with the two adjacent tubulins in the two adjacent filaments. Thus, the rate of the removal of the first tubulin is increased relative to that with no monomer bound to the first tubulin, which is consistent with the available experimental data.[24,28] In a word, the small depolymerase activity of the monomeric kinesin-8 is due to the slight tubulin curvature induced by the extensive contact of loop-2 with α-subunit of tubulin.

Taken together, in the model the depolymerase activity of the kinesin-8 motor is due mainly to the large internal force between the two heads bound to the curved tubulins near the MT plus end, which is facilitated by the presence of loop-2, while the ATP-binding-induced closure of the kinesin-8 head bound to the curved tubulin plays a minor role in the depolymerase activity.

4.3. Loop-2 has little effect on stepping activity of kinesin-8 motor on the MT lattice whereas has a facilitating effect on depolymerase activity of kinesin-8 motors at plus end

Our simulation results (Fig. 7) reveal that loop-2 differentially affects the dynamics of kinesin-8 motors during the processive stepping on the MT lattice and depolymerase activity at the plus end. In order to have a small internal force between the two heads bound to straight tubulins on the MT lattice, thus ensuring the very low probability of the defect generation during the processive stepping of the kinesin-8 motors on the MT lattice,[38] loop-2 has no influence on the backward-stretched NL of the leading kinesin-8 head. By contrast, in order to have a large internal force between the two heads bound to two adjacent curved tubulins at the MT plus end, loop-2 can interfere largely with the backward-stretched NL of the leading kinesin-8 head, thus facilitating the depolymerase activity of the kinesin-8 motors.

As seen from Fig. 7 for the ATP–Kip3–curved-tubulin complex, the counterclockwise rotation of loop-2 is coupled with that of loop-1. In other words, the counterclockwise rotation of loop-1 could facilitate the counterclockwise rotation of loop-2. Since loop-1 has no direct interference with the NL of the leading head, it is thus expected that the contribution of loop-1 on the depolymerization activity is via its role in facilitating the counterclockwise rotation of loop-2.

Acknowledgements

Project supported by the Science and Technology Research Program of Chongqing Municipal Education Commission (Grant No. KJQN202504529) and the General Program of Chongqing Natural Science Foundation (Grant No. CSTB2025NSCQ-GPX0833).

References

[1] Vale R D 2003 *Cell* **112** 467
[2] Lawrence C J, Dawe R K, Christie K R, *et al*. 2004 *J. Cell Boil.* **167** 19
[3] Miki H, Okada Y and Hirokawa N 2005 *Trends Cell Biol.* **15** 467
[4] Hirokawa N, Noda Y, Tanaka Y, *et al*. 2009 *Nat. Rev. Mol. Cell Bio.* **10** 682
[5] Vale R D, Reese T S and Sheetz M P 1985 *Cell* **42** 39
[6] Xie P 2024 *J. Phys. Chem. Lett.* **15** 3893
[7] Wang Y, Liu Y R, Wang P Y, *et al*. 2024 *J. Phys. Chem. B* **128** 1194
[8] Desai A, Verma S, Mitchison T J, *et al*. 1999 *Cell* **96** 69
[9] Hunter A W, Caplow M, Coy D L, *et al*. 2003 *Cell* **11** 445
[10] Wordeman L, Wagenbach M and von Dassow G 2007 *J. Cell Biol.* **179** 869
[11] Friel C T and Welburn J P 2018 *Biochem. Soc. Trans.* **46** 1665

[12] Gupta Jr M L, Carvalho P, Roof D M, *et al*. 2006 *Nat. Cell Biol.* **8** 913
[13] Howard J and Hyman A A 2007 *Curr. Opin. Cell Biol.* **19** 31
[14] Shrestha S, Hazelbaker M, Yount A L, *et al*. 2018 *Biomolecules* **9** 1
[15] Walczak C E, Gayek S and Ohi R 2013 *Annu. Rev. Cell Dev. Biol.* **29** 417
[16] Reilly M L and Benmerah A 2019 *Biol. Cell* **111** 79
[17] Xie P 2024 *Euro. Biophys. J.* **53** 339
[18] Jannasch A, Bormuth V, Storch M, *et al*. 2013 *Biophys. J.* **104** 2456
[19] Varga V, Helenius J, Tanaka K, *et al*. 2006 *Nat. Cell Biol.* **8** 957
[20] Su X, Qiu W, Gupta M L Jr, *et al*. 2011 *Cell* **43** 751
[21] Stumpff J, Du Y, English C A, *et al*. 2011 *Cell* **43** 764
[22] Varga V, Leduc C, Bormuth V, *et al*. 2009 *Cell* **138** 1174
[23] Wang D, Nitta R, Morikawa M, *et al*. 2016 *eLife* **5** e18101
[24] Arellano-Santoyo H, Geyer E A, Stokasimov E, *et al*. 2017 *Dev. Cell* **42** 37
[25] Du Y, English C A and Ohi R 2010 *Curr. Biol.* **20** 374
[26] Ciorita A, Bugiel M, Sudhakar S, *et al*. 2021 *Cytoskeleton* **78** 177
[27] Xie P 2024 *Adv. Protein Chem. Struct. Biol.* **141** 87
[28] Hunter B, Benoit M P M H, Asenjo A B, *et al*. 2022 *Nat. Commun.* **13** 4198
[29] Crevel I M T C, Lockhart A and Cross R A 1996 *J. Mol. Biol.* **257** 66
[30] Hancock W O and Howard J 1999 *Proc. Natl. Acad. Sci. USA* **96** 13147
[31] Sosa H, Peterman E J G, Moerner W E, *et al*. 2001 *Nature Struc. Biol.* **8** 540
[32] Uemura S, Kawaguchi K, Yajima J, *et al*. 2002 *Proc. Natl. Acad. Sci. USA* **99** 5977
[33] Cross R A 2016 *Biopolymers* **105** 476
[34] Benoit M P M H, Asenjo A B, Paydar M, *et al*. 2021 *Nat. Commun.* **12** 3637
[35] Fu Y B, Liu Y R, Wang P Y, *et al*. 2018 *J. Polymer. Sci. B: Polymer Phys.* **56** 297
[36] Xie P 2023 *J. Theor. Biol.* **571** 111556
[37] Gudimchuk N B, Ulyanov E V, O'Toole E, *et al*. 2020 *Nat. Commun.* **11** 3765
[38] Xie P 2025 *J. Theor. Biol.* **605** 112088
[39] Shi X X, Guo S K, Wang P Y, *et al*. 2020 *Proteins* **88** 545
[40] Pettersen E F, Goddard T D, Huang C C, *et al*. 2004 *J. Comput. Chem.* **25** 1605
[41] Hess B, Kutzner C, van der Spoel D, *et al*. 2008 *J. Chem. Theor. Comput.* **4** 435